sciendo

Acta Pharm. **73** (2023) 363–384
https://doi.org/10.2478/acph-2023-0034

Original research paper

Rosuvastatin effects on the HDL proteome in hyperlipidemic patients

ANA VAVLUKIS[1,*]
KRISTINA MLADENOVSKA[1]
KATARINA DAVALIEVA[2]
MARIJA VAVLUKIS[3]
ALEKSANDAR DIMOVSKI[1,2]

[1] *University Ss Cyril and Methodius Faculty of Pharmacy, 1000 Skopje RN Macedonia*

[2] *Macedonian Academy of Sciences and Arts, Research Center for Genetic Engineering and Biotechnology „Georgi D. Efremov", 1000 Skopje RN Macedonia*

[3] *University Ss Cyril and Methodius Faculty of Medicine, 1000 Skopje RN Macedonia*

Accepted August 7, 2023
Published online August 7, 2023

ABSTRACT

The advancements in proteomics have provided a better understanding of the functionality of apolipoproteins and lipoprotein-associated proteins, with the HDL lipoprotein fraction being the most studied. The focus of this study was to evaluate the HDL proteome in dyslipidemic subjects without an established cardiovascular disease, as well as to test whether rosuvastatin treatment alters the HDL proteome. Patients with primary hypercholesterolemia or mixed dyslipidemia were assigned to 20 mg/day rosuvastatin and blood samples were drawn at study entry and after 12 weeks of treatment. A label-free LC-MS/MS protein profiling was conducted, coupled with bioinformatics analysis. Sixty-nine HDL proteins were identified, belonging to four main biological function clusters: lipid transport and metabolism; platelet activation, degranulation, and aggregation, wound response and wound healing; immune response; inflammatory and acute phase response. Five HDL proteins showed statistically significant differences in the abundance (Anova ≤ 0.05), before and after rosuvastatin treatment. Platelet factor 4 variant (PF4V1), Pregnancy-specific beta-1-glycoprotein 2 (PSG2), Profilin-1 (PFN1) and Keratin type II cytoskeletal 2 epidermal (KRT2) showed decreased expressions, while Integrin alpha-IIb (ITGA2B) showed an increased expression after treatment with rosuvastatin. The ELISA validation of PFN1 segregated the subjects into responders and non-responders, as PFN1 levels after rosuvastatin were shown to mostly depend on the subjects' inflammatory phenotype. Findings from this study introduce novel insights into the HDL proteome and statin pleiotropism.

Keywords: proteomics, high-density lipoprotein, rosuvastatin, Profilin-1, phospholipid transfer protein, platelet factor 4 variant

Even though recent therapeutic advances have substantially reduced atherosclerotic cardiovascular disease (ASCVD) morbidity and mortality, it remains to be a substantial concern (1). Present-day evidence has hardened the lipid-retention hypothesis as a starting

*Correspondence; e-mails: ana.vavlukis@gmail.com

point in atherogenesis, with low-density lipoproteins (LDL) and other lipoproteins containing apolipoprotein (Apo)B as the principal participants (2).

Different pathological states, such as diabetes mellitus or dyslipidemia, functionally modify the endothelium, resulting in up-regulation of various chemotactic and adhesion entities. The enhanced vessel wall permeability allows LDL retention, due to the binding ability of ApoB100 to the proteoglycans in the extracellular space (3). Modified LDL particles, primarily by oxidation, deliver bioactive lipid moieties that lead to prolonged endothelial activation and leukocyte expression of multiple adhesion molecules, such as the vascular cell adhesion molecule-1 (VCAM-1), which attracts both T-cells and monocytes from the circulation. After the monocyte differentiation to macrophages, the expression of innate immunity pattern recognition receptors increases. Scavenger receptors mediate the macrophage inflow of oxidized LDL particles and apoptotic fragments, resulting in lipid build-up and the generation of foam cells (4). Oxidized-LDLs are known to trigger the recognition of toll-like receptors (TLRs), sending pro-inflammatory alerts. The enhanced expression of IL-1β, as the primary pro-inflammatory cytokine, leads to a cascade stimulation of various pro-inflammatory chemokines, cytokines, and transcription factors (nuclear factor-κB (NF-κB)), that potentiates the attraction of inflammatory and immune entities in the atherogenesis site (5).

Cholesterol disbalance is the primary lipid disorder related to atherosclerosis risk. The lipoproteins are macromolecular formations, with the primary role to carry cholesterol all around the body. Depending on their lipid/protein composition, they are divided into seven categories: chylomicrons, chylomicron remnants, very low-density lipoprotein (VLDL), intermediate-density lipoprotein (IDL), LDL, high-density lipoprotein (HDL), and lipoprotein(a) (Lp(a)) (6, 7).

HDLs represent a miscellaneous lipoprotein group, with particle variability regarding their size, density, charge, and protein-to-lipid make-up, mainly responsible for peripheral cholesterol efflux, with multiple anti-inflammatory, antioxidative, antithrombotic and antiapoptotic effects (6). Even though it was long thought that raising HDL-C levels would substantially decrease cardiovascular risk, recent evidence was not able to postulate a causal relation, shifting the HDL 'quantity' theory to a more functionality-based HDL 'quality' premise (1, 2, 8).

Numerous antilipemic agents are available nowadays, such as: inhibitors of 3-hydroxy-3-methylglutaryl-coenzyme A reductase (statins), sequestrants of bile acid, fibrates, inhibitors of cholesterol absorption, inhibitors of proprotein convertase subtilisin/kexin type 9 (PCSK9), inhibitors of adenosine triphosphate citrate lyase, and different gene-targeted treatments. Due to their proven efficacy and safety, statins are still the golden standard treatment in subjects carrying ASCVD risk, not only for their antilipemic actions, but for their diverse pleiotropic effects as well (1, 2).

With the mass spectrometry success, the use of next-generation proteomics is continuing to expand in the search for prospective disease markers and to elucidate the ASCVD origin mechanisms (9). Occurring proteomic data has allowed a better functional understanding of the lipoprotein proteome, with the protein-rich HDLs being most frequently examined (10). Proteins take up to 65 % of the molecular weight of the HDL fraction, presented mostly by apolipoproteins, proteins involved in lipid turnover, proteins involved in the inflammatory response, complement proteins, and different protease inhibitors (11). Roughly 1000 HDL-proteins have been reported by 45 studies published so far, with almost

250 proteins detected by no less than three different laboratories (12), stating big intra- and inter-individual variability in the results. Even though one would conclude that this heterogeneity translates to an indefinite number of HDL functions, a large number of the identified HDL proteins have much lower concentration levels compared to the levels of HDL itself, meaning that they persist in a specific HDL particle subset. By density gradient ultracentrifugation, two main subfractions, HDL2 (larger) and HDL3 (smaller), can be separated, with HDL2 being the more atheroprotective fraction. By gel electrophoresis, HDL particles can be divided into HDL2b, HDL2a, HDL3a, HDL3b, and HDL3c subclasses. 2D electrophoresis distinguishes lipid-poor pre-β-HDL and cholesterol ester-containing α-HDL. Therefore, one would postulate that the HDL proteome is the principal regulator of the HDL biochemical profile.

Considering the previously stated, the aims of the introduced study were to evaluate the HDL proteome in dyslipidemic subjects carrying a low-to-moderate cardiovascular risk, but without an established cardiovascular disease, as well as to test whether rosuvastatin treatment alters the HDL proteome, thus possibly affecting its functional properties.

EXPERIMENTAL

Subjects and study design

For the objectives of this study, 47 adult ambulatory patients (aged 55.7 ± 8.1 years, 25 women, 22 men) from the University Clinic of Cardiology – UKIM, Skopje were included. 10 of the subjects were included in the discovery group (aged 56.9 ± 5.0 years, 5 women, 5 men) and 37 of the subjects were included in the validation group (aged 55.4 ± 8.8 years, 20 women, 17 men). Subjects were part of a bigger cohort for a national study intended to evaluate rosuvastatin pleiotropic effects, in terms of its anti-inflammatory, antioxidative effects, and effects on lipoprotein proteomics. The presented study was conducted in accordance with the Declaration of Helsinki and the ICH GCP guideline (CPMP/ICH/135/95). A written informed consent form was signed by every subject included prior to starting the study. Every study document requiring previous ethical approval (the clinical study protocol, the informed consent, and all other subject information documents) was reviewed and approved by the Ethics Committee for Human Research (Faculty of Medicine – UKIM, Skopje, RN Macedonia), document number 03-3192/9, issued on 7th of September 2018.

Subjects were statin "naïve", with primary hypercholesterolemia or mixed dyslipidemia. Their selection was done in order to achieve homogeneity of the group in terms of gender, age, traditional risk factors [non-smokers, with diagnosed hypertension, previously diagnosed, untreated hyperlipidemia (total cholesterol (Chol) > 6.2 mmol L^{-1}, LDL-C > 4.1 mmol L^{-1}, TG > 2.3 mmol L^{-1}) and a normal glucose status (3.9–5.6 mmol L^{-1})], concomitant pharmacological therapy (acetylsalicylic acid, bisoprolol, perindopril) and the intensity of the treatment response to rosuvastatin therapy (30–50 % Chol reduction, 40–60 % LDL-C reduction, and 1–3 % reduction in the total SCORE risk of CVD). All clinical and biochemical parameters that were followed in the study cohort can be found in Supplementary Table SI.

Preselection of the patients was done based on their physical status, medical history, and biochemical parameter results (hematology, electrolyte status, protein status, and

thyroid measures) from blood samples drawn at the screening clinical visit. Exclusion criteria were defined as follows: (rosuva)statin hypersensitivity, prior lipid-modifying treatment, muscle pain, myopathy or rhabdomyolysis, diseases affecting the heart, kidney, or liver, systemic inflammatory diseases, autoimmune diseases, diagnosis of cancer within the previous 5 years, HIV-positive subjects, pregnant and/or nursing women, subjects who have donated blood in the previous 4 weeks, 1.5-fold increased transaminases levels (above upper referent limits), 5-fold increased creatinine kinase levels (above upper referent limit) or clearance of creatinine falling below 30 mL min^{-1}.

Subjects included in the study were given 20 mg/day rosuvastatin, for a period of 12 weeks. Subject compliance was concluded as satisfactory in the case of a minimum of 80 % dosage units administered. At the study start-up, and after 12 weeks of treatment with rosuvastatin, 10.0 mL of venous blood was drawn from each subject. Given that blood samples were drawn from each participant at study entry and during treatment, each participant acted as their own control. After centrifugation at 3000 rpm/15 min, the separated plasma was stored and kept at –80 °C until further analysis. Samples were later transported, at –80 °C, to the Cardiovascular ICCC-Program, Research Institute Hospital de la Santa Creu y Sant Pau, IIB-Sant Pau, 08025 Barcelona, Spain, for lipoprotein separation and isolation. Lastly, the HDL proteomic mapping was done at the Research Center for Genetic Engineering and Biotechnology „Georgi D. Efremov", Macedonian Academy of Sciences and Arts.

Lipoprotein isolation

HDL (density 1.063–1.210 g mL^{-1}) was isolated from plasma using sequential ultracentrifugation, according to the methods proposed by Havel *et al.* (1955) (13) and De Juan-Franco *et al.* (2009) (14). More precisely, the plasma samples were adjusted to a density of 1.019 g mL^{-1}, using a concentrated potassium bromide solution, after which they were centrifuged at 50,000 rpm, for a period of 18 h, using a Beckman L-60 ultracentrifuge with a fixed-angle type 50.4 Ti rotor (Beckman, USA). After aspiration of the top tubal layer (VLDL and IDL), the density of the remaining aliquot was further adjusted to 1.063 g mL^{-1}, and centrifugated again at 50,000 rpm, for a period of 20 h. After the aspiration of the top tubal layer (LDL), the density of the infranatant was adjusted to 1.210 g mL^{-1}, and the aliquots were finally centrifuged at 50,000 rpm, for a period of 24 h at 4 °C, allowing separation of HDL from the remnant lipoprotein-deficient serum. The obtained HDL fraction was dialyzed for 24 h, using an 1X phosphate buffer. Protein quantification was done using the Bicinchoninic Acid (BCA) protein colorimetric assay (Pierce, Thermo Fischer Scientific, USA), finally adjusting the obtained HDL samples to a protein concentration of 100 μg mL^{-1}, waiting for further mass spectrometry analysis.

Lipoprotein preparation for Liquid Chromatography-tandem Mass Spectrometry (LC-MS/MS)

The RapiGest protocol was used, with some minor modifications (15, 16). In summary, 100 μL of each individual HDL sample was mixed with 150 μL methanol and 38 μL chloroform. After 1 min of vortexing and 5 min of centrifugation at 5,000×g, the proteins remained at the interface between the hydrophilic and the lipophilic layer. After removal

of the upper hydrophilic layer, 112 μL of methanol was added, further centrifuging the samples for 5 min at 16,000×g, to obtain the protein pellets. The proteins were further dissolved in 50 mmol L^{-1} ammonium bicarbonate, previously mixed with the 0.1 % RapiGest TM detergent (Waters Corp.), maintaining a 2.5:1 *m*/*V* ratio. After the addition of dithiothreitol (0.12 μmol for every 50 μg protein), the aliquots were sonicated and boiled for 5 min. The interim protein concentration of the samples was measured using the Bradford assay. A sample portion equivalent to 20 μg of protein was diluted to 35 μL, using a 0.1 % RapiGest in 50 mmol L^{-1} ammonium bicarbonate solution, and heated at 80 °C for a period of 15 min. Pools of the samples were later reduced for 30 min in 5 mmol L^{-1} dithiothreitol, maintain a temperature of 60 °C, and then alkylated for 30 min in 15 mmol L^{-1} iodoacetamide, at room temperature and protected from light. The samples were than spiked with trypsin (TRYPSEQM-RO ROCHE) (at a ratio of 1:100 trypsin/protein) and incubated for 12 h at 37 °C. After the digestion was finished 5 % trifluoroacetic acid was added (to obtain a content of 0.5 %), further incubating the samples for 90 min at 37 °C. Following a 30 min centrifugation at 14,000 rpm (6 °C), obtained supernatants were moved to Waters Total Recovery vials and water diluted to obtain a concentration of 0.4 μg μL^{-1} protein. Alcohol dehydrogenase (ADH) digest was used as an internal standard. The samples' final concentration was 200 ng μL^{-1} of protein and 25 fmol μL^{-1} of ADH.

Nano- LC-MS/MS using label-free data-independent MS^E acquisition

A label-free LC-MS/MS protein profiling was performed using an ultra-performance liquid chromatography system ACQUITY UPLC® M-Class (Waters Corporation), coupled with a SYNAPT G2-Si High Definition Mass Spectrometer (Waters Corporation) equipped with a T-Wave-IMS device. Data was obtained using classical MS^E acquisition (17).

For each sample analyzed, quality assurance and protein quantification were done by running one test run in the MS^E mode and processing the obtained initial data using the ProteinLynx Global Server (PLGS, version 3.0.3, Waters Corp., Milford, MA, USA). Optimal column loading was determined by testing a pooled sample, from 100 to 300 ng per run, with subsequent processing in the ProteinLynx Global Server. Samples were run with an optimal column load of 250 ng (18).

The LC-MS/MS sample analysis was done according to the parameters postulated by Davalieva *et al*. (2021) (16). "Peptides were trapped on an ACQUITY UPLC M-Class Trap column Symmetry C18, 5 μm particles, 180 μm × 20 mm, (Waters Corporation), for 3 min at 8 μL min^{-1} in 0.1 % solvent B (0.1 % (*V*/*V*) formic acid in acetonitrile)/99.9 % solvent A (0.1 % (*V*/*V*) formic acid, aqueous). The injection was followed by a needle wash with 1 % acetonitrile, and 0.1 % trifluoroacetic acid. Peptide separation was done on ACQUITY UPLC M-Class reverse phase C18 column HSS T3, 1.8 μm, 75 μm × 250 mm (Waters Corporation), at a flow rate of 300 nL min^{-1} using a 90 min multistep concave gradient for nanoLC separation. Briefly, the column was equilibrated for 5 min at 1 % B, and then solvent B was increased in a 90-min gradient between 5 and 40 %, post-gradient cycled to 95 % B for 7 min, followed by 8 min post-run equilibration at 1 % B. The analytical column temperature was set to 55 °C.

Lock mass compound Glu-1-Fibrinopeptide B (EGVNDNEEGFFSAR) was delivered by the auxiliary pump of the LC system at 500 nL min^{-1} to the reference sprayer of the NanoLockSpray source of the mass spectrometer. The concentration of Glu-1-Fibrinopeptide B in the reference solution (50 % acetonitrile, 0.1 % formic acid) was 100 fmol μL^{-1}. The

lock mass spectrum of doubly charged Glu-1-Fibrinopeptide B (*m*/*z* 785.8426) was produced every 45 s.

Spectra were recorded in resolution positive ion mode with a typical resolving power of at least 25,000 FWHM (full width at half maximum) and sensitivity of > 7000 TDC equivalent counts/sec for the double charged Glu-1-Fibrinopeptide B ion (*m*/*z* 785.8426) infused directly at a concentration of 100 fmol μL^{-1}. The time-of-flight analyzer of the mass spectrometer was calibrated with a Glu-1-Fibrinopeptide B in the *m*/*z* range 50–2000. Source settings included a capillary voltage of 3.2 kV, extraction cone at 4 V, sampling cone at 35 V, and source temperature of 80 °C. The cone gas N2 flow was 30 L h^{-1}. Analyzer settings included quadrupole profile set at auto with mass 1 as 1.25 Ma (dwell time 25 % and ramp time 75 %) and mass 2 as 0.17 Mb. The Step Wave settings in TOF acquisition mode were the following: wave velocity of 20 m s^{-1} and wave height 15 V for the StepWave 1 and StepWave 2, and wave velocity of 300 m s^{-1} and wave height 5 V for the Source Ion Guide. The Step Wave settings in TOF mobility acquisition mode were the following: wave velocity of 300 m s^{-1} and wave height 15 V, 15 V, and 1 V for the StepWave 1 and StepWave 2, and Source Ion Guide, respectively. For IMS, a wave height of 40 V was set. Traveling wave velocity was ramped from 900 to 450 m s^{-1} over the full IMS cycle. Wave velocities in the trap and transfer cell were set to 311 and 175 m s^{-1}, respectively, and wave heights to 4 V. Spectra were collected over the mass range 50–2000 *m*/*z*, with a scan time of 0.5 s. The collision energy was held at 4 V for the low-energy scan and ramped from 17 to 45 V for the high-energy scan (ref. 16, p. 6–7).

LC-MS/MS data analysis

Data processing, protein identification, and quantification were done using Progenesis QIP version 4.1 (Nonlinear Dynamics, Waters Corp., USA). Obtained data were searched against the UniProtKB/Swiss-Prot database (20,407 proteins as of March, 2023), to which the ADH sequence was added (UniProt accession number P00330). Low energy (LE) and high energy (HE) threshold settings were set on auto mode. The mass tolerances for the precursor and the fragment ions were established automatically in the database mining process. The range of RMS error was ± 5 ppm for the precursor ion, and ± 10 ppm for the fragment ion. Search filters were set as follows: one fixed modification – carbamidomethyl cysteine (+57.02 Da), maximum of one missed trypsin cleavage, and one variable modification – oxidized methionine (+15.99 Da). Peptide identification was based on at least 2 fragment ion matches, while protein identification was based on at least 5 fragment ion matches and a minimum of 1 peptide match. A 1 % protein false discovery rate was used as a threshold for database search. The quantification was based on the following inputs: ADH, P00330; concentration, 25 fmol μL^{-1}. All run protein abundances were normalized using the least variable run. Relative quantification was based on non-conflicting peptides only. Positive identification and quantification of proteins were based on two or more peptide matches per identification, and at least one unique peptide for quantification.

Proteomics data analysis

Proteins with differential abundance before and after treatment were considered with fold change ≥ 1.2 and Anova ≤ 0.05. For an overview of the identified protein localization,

and molecular and biological function, the UniProt Knowledgebase (UniProtKB) and the Gene Ontology (GO) database were used. The DIGE GOnet tool was used for an interactive GO analysis, using an FDR ≤ 0.0001. A network analysis was done using the STRING database, in order to investigate for possible interactions between the identified proteins, primarily in the context of their biological function. Protein expression and localization were evaluated using the Human Protein Atlas (HPA) Database, version 20.1 (http://www.proteinatlas.org/).

ELISA validation of proteomics data

Two differentially expressed proteins were quantitatively evaluated using commercial ELISA kits (Elabscience®, Elabscience Biotechnology Inc., USA), in order to validate the obtained MS proteomics data. Platelet factor 4 variant (PF4V1) was validated with the Human PF4V1(Platelet Factor 4 Variant 1) ELISA Kit (Elabscience®, catalogue number: E-EL-H2217), while Profilin-1 (PFN1) was validated with the Human PFN1(Profilin 1) ELISA Kit (Elabscience®, catalogue number: E-EL-H2302).

Statistical analysis

The obtained pre-/post-treatment concentration values were statistically analyzed with the Statistica for Windows software, Version 19.0 (SPSS Inc., USA). Paired samples *t*-test and Wilcoxon Signed Rank test were used for comparative analysis. Univariate and multivariate logistic regression analyses were performed, with statistical significance defined as $p \leq 0.05$.

RESULTS AND DISCUSSION

Overview and analysis of the proteomics data

The Progenesis QIP comparative analysis concluded the identification of 83 proteins with quantitative values, based on 1077 peptide identifications. Following the removal of all proteins which were identified on the basis of only one peptide match, the final HDL proteome contained a total of 69 proteins identified on the basis of ≥ 2 peptide matches (Supplementary Table SII).

To gain insight into the cellular localization, the reported molecular functions, and their involvement in different biological processes, all identified HDL proteins were analyzed by their GO annotations (Fig. 1). In terms of cellular localization, most of the proteins were localized in the extracellular space (61 proteins), as part of the blood microparticles (26 proteins) and lipoprotein particles (20 proteins) (Fig. 1a). In terms of molecular function, most of the proteins were involved in signaling receptor binding (22 proteins) and molecular function regulation (18 proteins) (Fig. 1b). Regarding their biological function, most of the proteins were involved in localization (52 proteins), response to stimuli (52 proteins), transport (46 proteins) and cellular organization (42 proteins) (Fig. 1c).

To better visualize their dispersion regarding the localization, molecular and biological involvement of the proteins, a GOnet interactive GO analysis was done (Fig. 2). 19 HDL

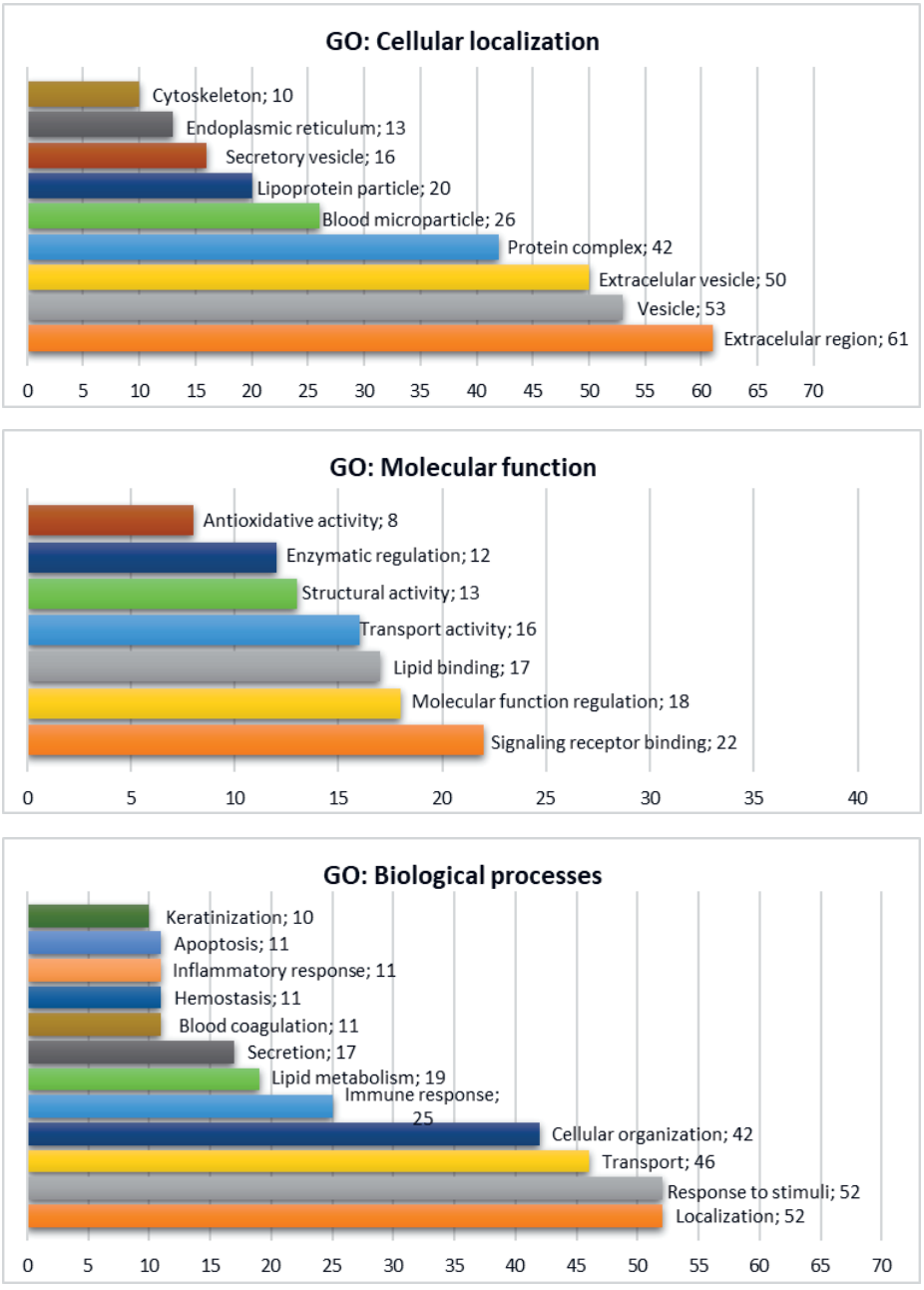

Fig. 1. GO Annotations of the identified HDL proteins using the Uniprot and EBI QuickGO databases. The y-axis shows the GO term that annotates a given set of proteins; the x-axis shows the number of detected GO annotations for a given GO term.

proteins, 4 IDL proteins, 11 VLDL proteins, 5 LDL proteins, and 7 chylomicron proteins were identified (Fig. 2a). In terms of their molecular function, most of the proteins were included in lipid binding (in the role of receptors) (17 proteins), of which 7 cholesterol-binding proteins were identified, lipid transport (10 proteins), lecithin-cholesterol acyltransferase activation (4 proteins), antioxidative activity (8 proteins), and signal transduction (22 proteins) (Fig. 2b). In terms of their involvement in biological processes, most of the detected proteins were involved in the lipid metabolism, such as plasma lipoprotein

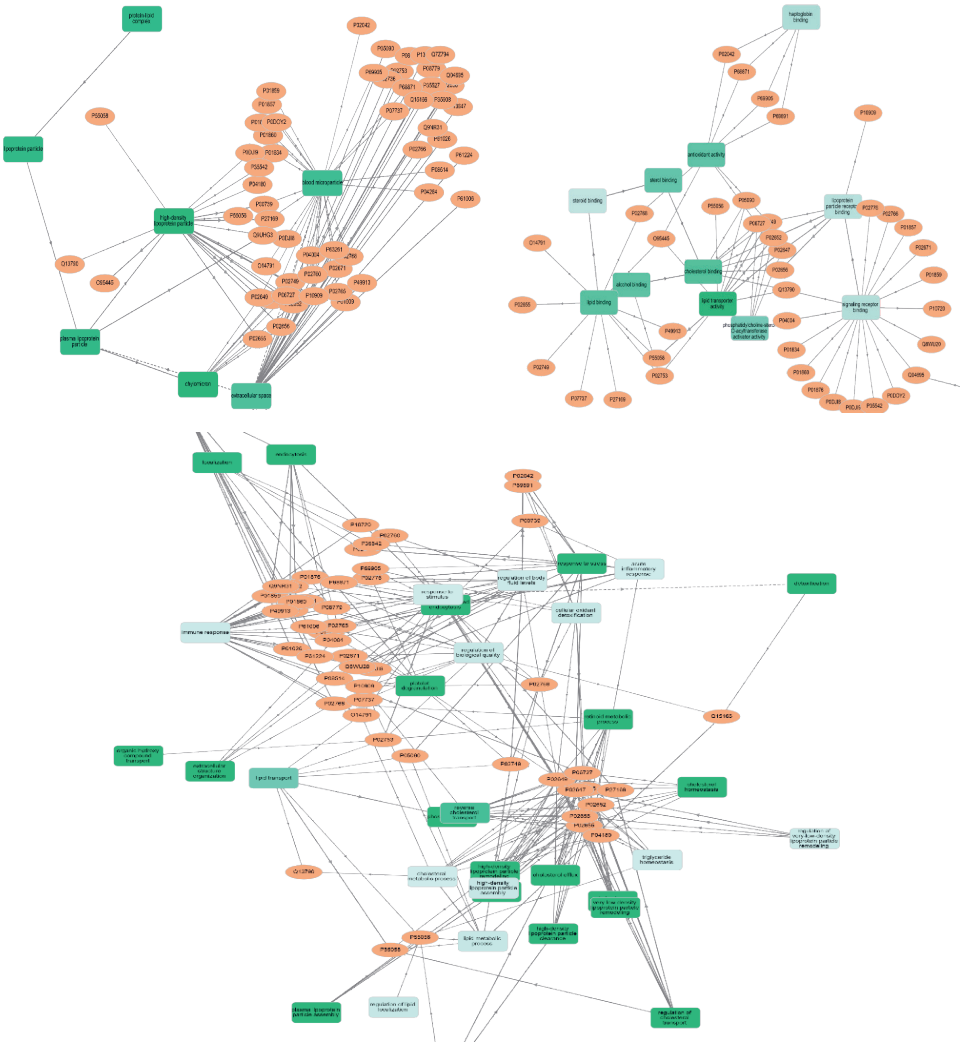

Fig. 2. GOnet interactive GO analysis of the identified HDL proteins: a) cellular localization, b) molecular functions, c) biological processes. Proteins are represented with ellipses, while the rectangles represent GO terms.

clearance (7 proteins), formation of lipoprotein particles (8 proteins), remodeling of lipoproteins (21 proteins), lipid transport (16 proteins) and cholesterol efflux (7 proteins). 7 proteins were involved in the detoxification process, 8 proteins were part of the cellular oxidative detoxification, 29 proteins participated in vesicular transport, 22 proteins participated in the immune response, of which 7 proteins were identified as part of the acute inflammatory response, and 9 proteins involved in the platelet degranulation process (Fig. 2c).

Although ApoA1 and ApoA2 present nearly 90 % of the HDL protein abundance, the quantum of reported HDL-proteins has been in constant increase in the last decade. Ronsein G et al. analyzed nearly 40 HDL-proteomic studies, reporting a sum of 566 HDL-proteins (19). ApoA1 and ApoL were the sole HDL-proteins reported by all studies, with just 21 HDL-proteins reported by 75 % of the analyzed reports, probably as a result of the difference in isolation methods and mass spectrometry programs used for HDL-proteome analysis. Since 2023, the HDL Proteome Watch Database combines 51 proteomics studies of HDL, with 1030 reported and 285 "most probable" HDL-proteins (20). Of the identified

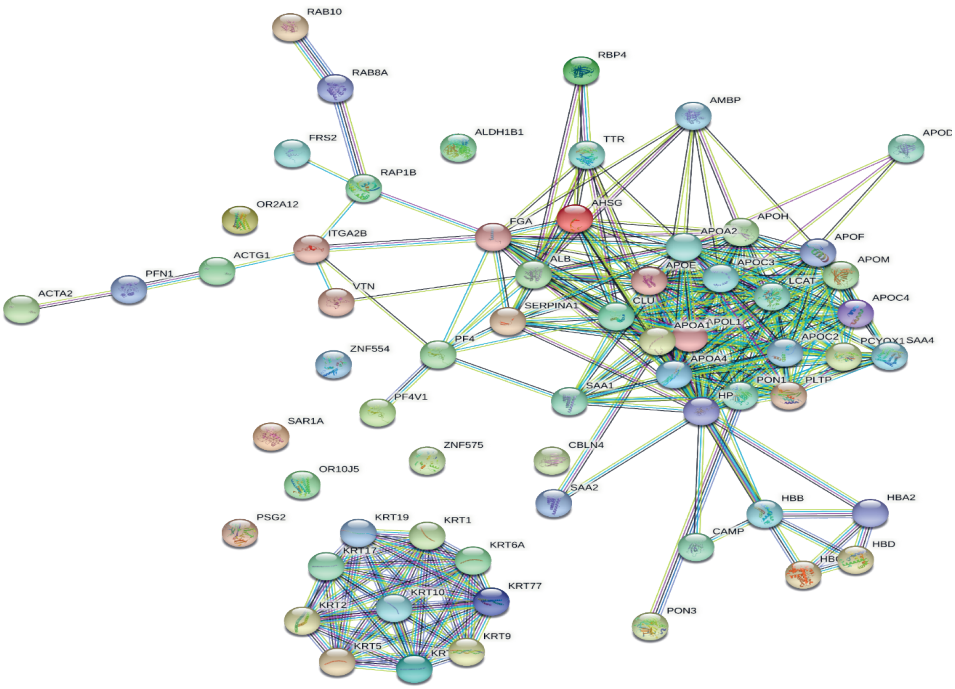

Fig. 3. STRING analysis of the interactions among the identified HDL proteins. Legend: The circles represent the identified proteins (with their 3D structure); the lines represent protein-protein interactions (known interactions: light blue lines represent interactions from curated databases; pink lines represent experimentally determined interactions/predicted interactions: green lines represent interactions predicted by gene neighborhood; red lines represent interactions predicted by gene fusions; dark blue lines represent interactions predicted by gene co-occurrence/others: yellow lines represent interactions by text mining; black lines represent interactions by co-expression; purple lines represent interactions by protein homology).

HDL proteins in our study, 59 (85.5 %) proteins were consistent with the HDL Proteome Watch Database (regarding the "most probable" HDL proteins). The other 10 (14.5 %) proteins that were not identified in previous HDL proteomic studies are: Zinc Finger Protein 554 (ZNF554) and Zinc Finger Protein 575 (ZNF575), involved in DNA repair and cell migration; Olfactory receptor 10J5 (OR10J5) and Olfactory receptor 2A12 (OR2A12), responsible for detecting odorants in the olfactory receptor neurons; Cerebelin 4 (CBLN4), included in the formation and maintenance of inhibitory gamma-aminobutyric acid synapses, primarily in the central nervous system; Fibroblast Growth Factor Receptor Substrate 2 (FRS2), which mediates the binding of the fibroblast growth factor to its receptors, inducing cell proliferation, migration and differentiation; Pregnancy Specific Beta-1-Glycoprotein 2 (PSG2), pregnancy-specific protein involved in fetal development; Ras-related protein Rab10 (RAB10) and Ras-related protein Rab8A (RAB8A), involved in the intracellular protein membrane transport; PF4V1, an angiogenesis inhibitor released by activated platelet alpha-granules (UniProtKB).

Given that numerous proteins participate in more than one biological function of HDL, a network analysis using STRING was done in order to evaluate possible functional protein-protein interactions. Fig. 3. provides an interactive representation of the STRING analysis of the 69 identified HDL proteins, by selecting those protein-protein interactions with a high confidence score (0.700). Keratins formed a separate protein cluster, which showed no interaction with the other identified proteins. Because keratins are generally considered contaminants of lipoprotein samples (8), they were not considered in the following discussion.

A protein enrichment analysis identified four major biological functions of the identified HDL proteins (PPI enrichment $p = 0.00071$), which are shown in Fig. 4. Those are: a) Proteins involved in lipid transport and metabolism, and formation and clearance of lipoprotein particles; b) Proteins involved in platelet activation, degranulation and aggregation, the complement cascade, the coagulation cascade, wound response and wound healing (haemostasis); c) Proteins involved in the immune response; d) Proteins involved in the inflammatory response and acute phase response.

The obtained results from the protein-protein interaction analysis are in concordance with previous observations (19, 20). As anticipated, most of the identified HDL proteins were involved in lipid assembly, metabolism, binding, and transport, presented by the typical HDL apolipoproteins, which have been profoundly examined (21). HDL particles have been seen to carry substantial masses of different proteases and protease inhibitors, primarily serine proteases and SERPINS, like alpha-1-antitrypsin, or the phospholipid-transfer protein (22, 23). HDL proteins such as ApoA4 and serum amyloid A isoforms 1, 2, and 4 have already set roles in the inflammatory response (21). Multiple HDL-proteomic analyses have reported numerous HDL proteins as a part of innate immunity, such as ApoL1 and haptoglobin-related proteins (24). ApoA4 has the ability to bind to integrin αIIbβ3 on the platelet surface, allowing HDL to inhibit one of the primary thrombosis steps (25). Nearly half of the presently known complement proteins have been identified as part of the HDL-proteome, pointing to the role of HDL in the complement cascade (26). Taking into consideration the currently available evidence in terms of functionality, HDL exists as an extracellular destination of numerous proteins involved in human biology, as well as its pathology.

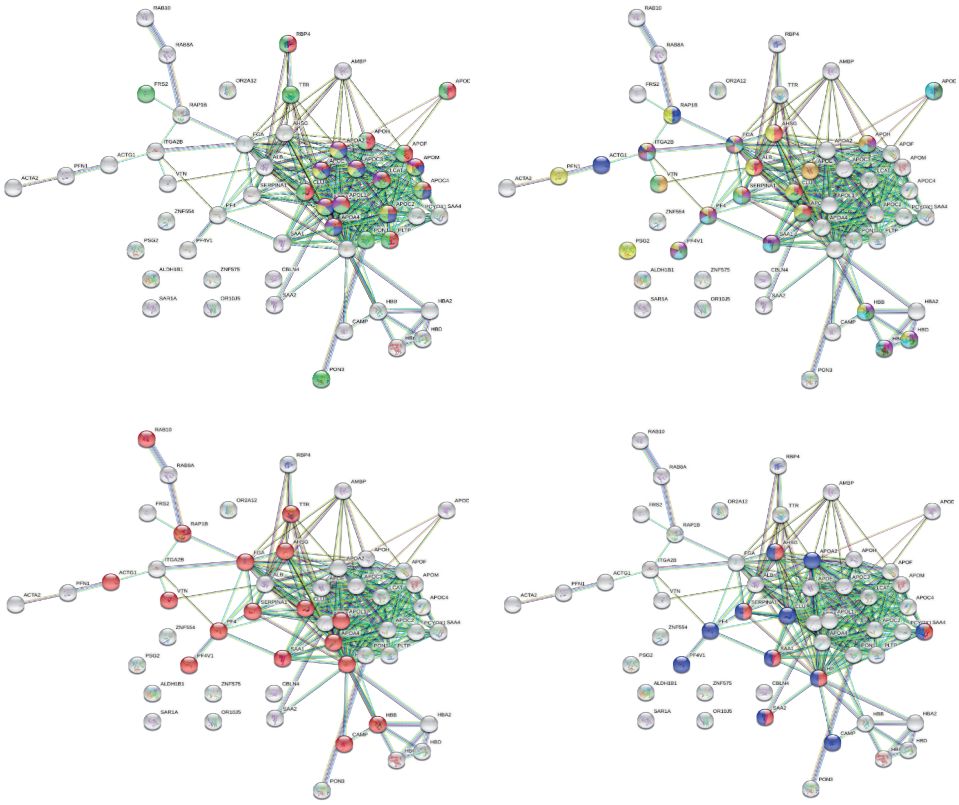

Fig. 4. STRING analysis of the identified HDL proteins according to the four most common GO annotations of the protein biological functions: a) proteins involved in lipid transport (green) and metabolism (red), and formation (pink and violet), and clearance (yellow) of lipoprotein particles; b) proteins involved in platelet activation (yellow), degranulation (red) and aggregation (green), the complement cascade (pink), the coagulation cascade (light blue), wound response (blue) and wound healing (hemostasis) (light blue and blue); c) proteins involved in the immune response (red); d) proteins involved in the inflammatory response (blue) and acute phase response (red).

Proteins with differential abundance after rosuvastatin treatment

Out of the 69 identified proteins with the MS^E data acquisition mode, five HDL proteins showed statistically significant differences in the abundance (Anova ≤ 0.05), before and after rosuvastatin treatment. Platelet factor 4 variant (PF4V1), Pregnancy-specific beta-1-glycoprotein 2 (PSG2), Profilin-1 (PFN1), and Keratin type II cytoskeletal 2 epidermal (KRT2) showed decreased expressions after treatment with rosuvastatin. On the other hand, Integrin alpha-IIb (ITGA2B) showed an increased expression after treatment with rosuvastatin. Table I. shows the differentially expressed HDL proteins after rosuvastatin treatment with their GO annotations.

Table I. Differentially expressed HDL proteins before and after rosuvastatin treatment, and their Gene Ontology annotations

Gene	Protein name	Anova (*p*)	Ratio (BEFORE/ AFTER)	GO (cellular component)	GO (molecular function)	GO (biological process)
PF4V1	Platelet factor 4 variant	1.13E-03	1.43	extracellular space	chemokine activity; heparin-binding	chemokine-mediated signaling pathway; immune response; inflammatory response; leukocyte chemotaxis; neutrophil chemotaxis; platelet activation
ITGA2B	Integrin alpha-IIb	1.84E-02	0.61	blood microparticle; extracellular exosome; integrin complex; plasma membrane; platelet alpha granule membrane	extracellular matrix binding; fibrinogen binding; metal ion binding	integrin-mediated signaling pathway; platelet aggregation; platelet degranulation; positive regulation of leukocyte migration; regulation of megakaryocyte differentiation
PSG2	Pregnancy-specific beta-1-glycoprotein 2	2.41E-02	3.16	extracellular region		cell migration; female pregnancy
PFN1	Profilin-1	4.15E-02	1.21	blood microparticle; cytoplasm; extracellular exosome; focal adhesion; membrane; nucleus	actin binding; cadherin binding; RNA binding	actin cytoskeleton organization; positive regulation of ATPase activity; positive regulation of epithelial cell migration; Wnt signaling pathway; planar cell polarity pathway
KRT2	Keratin_ type II cytoskeletal 2 epidermal	4.20E-02	1.22	cytosol; extracellular exosome; extracellular keratin filament	cytoskeletal protein binding; structural constituent of cytoskeleton and skin epidermis	cornification; epidermis development; keratinization

Profilin-1 (PFN1) is one of the first identified actin-binding cytosolic proteins. It also stimulates the polymerization of globular actin monomers (G-actin) into filamentous actin (F-actin). PFN1 is known to relate to numerous ligands, participating in different signaling pathways. Although it is primarily an intracellular protein, there is experimental evidence that various cells can release smaller portions into the extracellular space, making it part of the systemic circulation where PFN1 interacts with different entities intricated in endocytosis, autophagy, and gene transcription (27, 28). Studies have shown that atherosclerosis and chronic inflammation up-regulate PFN1 in the endothelium and the vascular smooth muscles. Clinical evidence shows enhanced PFN1 expression in atherosclerotic plaques, with a positive association between the levels of PFN1 and the existence of a pro-inflammatory setting with notable macrophage permeation (29, 30). Both healthy and atherosclerosis blood samples have shown the presence of PFN1, with increased PFN1 circulation levels associated with more severe disease (30). Additionally, enhanced PFN1 expression in the endothelium has been associated with a proportionate extracellular secretion increase. Numerous reports have also postulated the importance of PFN1 in angiogenesis. Increased expression of vascular endothelial growth factor results in increased PFN1 phosphorylation, which in turn increases its ability to bind to actin, thus stimulating angiogenesis (28). Despite these theories, the precise mechanisms by which PFN1 engages in the pathogenesis of CVD remain unclear. Although there are proteomic studies that have identified PFN1 as part of the HDL proteome (20), no evidence exists as to whether PFN1 uses HDL only as a plasma transporter or has a specific biological function within. This is the first clinical study to show the effect of statins on PFN1 expression. Considering its proposed pro-atherogenic effect, the reduction in its HDL expression indicates novel antiatherogenic effects of rosuvastatin.

Platelet factor 4 variant (PF4V1) results from a highly homologous *PF4* gene, made by duplication. The complete human PF4V1 consists of 104 amino acids, with four additional arginine residues as compared to PF4, which is responsible for its localization and its secretion method. While PF4 resides in the cytoplasm and is released only after the activation of protein kinase C, PF4V1 is continuously and constitutively produced and secreted in the circulation. The precise platelet localization of PF4V1 is still unknown. Platelets secrete both proteins, with PF4V1 being secreted nearly to a 50 times lesser extent as compared to PF4 (31). Only vascular smooth muscle cells secrete exclusively PF4V1 (32). The mature PF4V1 consists of 70 amino acids, with three different amino acids in the carboxy-terminal end of PF4, which affects its secondary structure and results in a notably decreased affinity for heparin, heparan, and chondroitin sulfate. CXCR3 has been identified as a functional receptor for PF4V1, which participates in its angiostatic and chemotactic actions. PF4V1 has a more potent chemotactic potential for T and NK cells, as compared to PF4, with a lower affinity for monocytes and neutrophils. Its enhanced angiostatic potential leads to substantial inhibition of the IL-8-stimulated endothelial chemotaxis and the vascular endothelial growth factor-stimulated angiogenesis (33). PF4V1 forms very stable homodimers, resulting in prolonged plasma half-lives (32). Although PF4V1 has no effect on monocyte differentiation, it induces the monocyte expression of several pro-inflammatory chemokine receptors, which enhances the chemotactic monocyte response (34). As compared to PF4, PF4V1 has a weaker pro-coagulant effect, but a stronger pro-inflammatory effect. The role of PF4V1 in vascular pathology, and the processes associated with atherosclerosis, has not yet been investigated. After an intensive search of the available scientific databases, we consider this to be the first proteomic study to identify PF4V1 as part of the

HDL proteome and to show the effect of statins on the HDL expression of PF4V1. Although PF4V1 is thought to have pro-inflammatory and pro-thrombotic effects, further research is needed to determine whether reducing PF4V1 expression by rosuvastatin is beneficial.

Integrin alpha-IIb (ITGA2B) is a surface receptor found in platelets, megakaryocytes, fat cells, and basophils. It binds primarily to fibrinogen, fibronectin, vitronectin, and von Willebrand factor (35). The receptor resides in a low-affinity circulatory state, which upon activation with thrombin and/or epinephrine coverts to a high-affinity conformation. The receptor is included in the adhesion and aggregation of platelets. Given that integrins are integral membrane proteins, their identification and significant differential expression, within the HDL proteome, is surprising. Given that it is primarily localized on the platelet surface this result probably indicates platelet contamination of the lipoprotein isolates. This finding requires further research, which was beyond the scope of this study.

Keratin type II cytoskeletal 2 epidermal (KRT2) is a type II cytokeratin primarily localized in the upper spinous and granular suprabasal epidermal layers, leading to terminal cornification and keratinization (UniProtKB). Because skin keratins are considered contaminants from the process of lipoprotein isolation and preparation, this protein was not considered for further analysis (36).

Pregnancy-specific beta-1-glycoprotein 2 (PSG2) is a carbohydrate-protein mixture, specifically present during pregnancy. As an immunoglobulin, it mainly acts as an immunomodulator for fetal protection during the growth and development phases (UniProtKB). Given the fact that pregnant women were not included in the study, as well as the small peptide number/unique peptides on which its identification and quantification are based, it is considered to be a protein mismatch.

Validation of selected differentially expressed HDL proteins with ELISA

Given the previously discussed, PF4V1 and PFN1 were further quantitatively evaluated by ELISA, in order to independently validate the obtained proteomic results and to accurately quantify their concentrations before and after rosuvastatin treatment. Both proteins are thought to have pro-atherogenic effects, so the observed reduction in their HDL expression with rosuvastatin indicates novel antiatherogenic effects of statin treatment and was therefore selected for subsequent validation.

The ELISA quantitative evaluation of the change in the levels of PF4V1 in the examined population, by comparing the obtained concentration results before and after treatment, did not show any statistically significant difference. In the three subjects in which the protein was detected (according to the test detection limit), a significant reduction in the level of PF4V1 was observed after treatment, compared to the values obtained before treatment, in each subject respectively ($p > 0.05$ with paired samples t-test and Wilcoxon Signed Rank Test) (Fig. 5a).

The ELISA quantitative evaluation of the change in the levels of PFN1 in the examined population, by comparing the obtained concentration results before and after treatment, did not show any statistically significant difference ($p > 0.05$ with paired samples *t*-test and Wilcoxon Signed Rank Test) (510.7 *vs.* 442.1 pg PFN1/mg HDL protein) (Fig. 5b).

Although no statistically significant difference was observed in the studied population for the ELISA validation of Profilin-1, it was observed that there was a segregation of

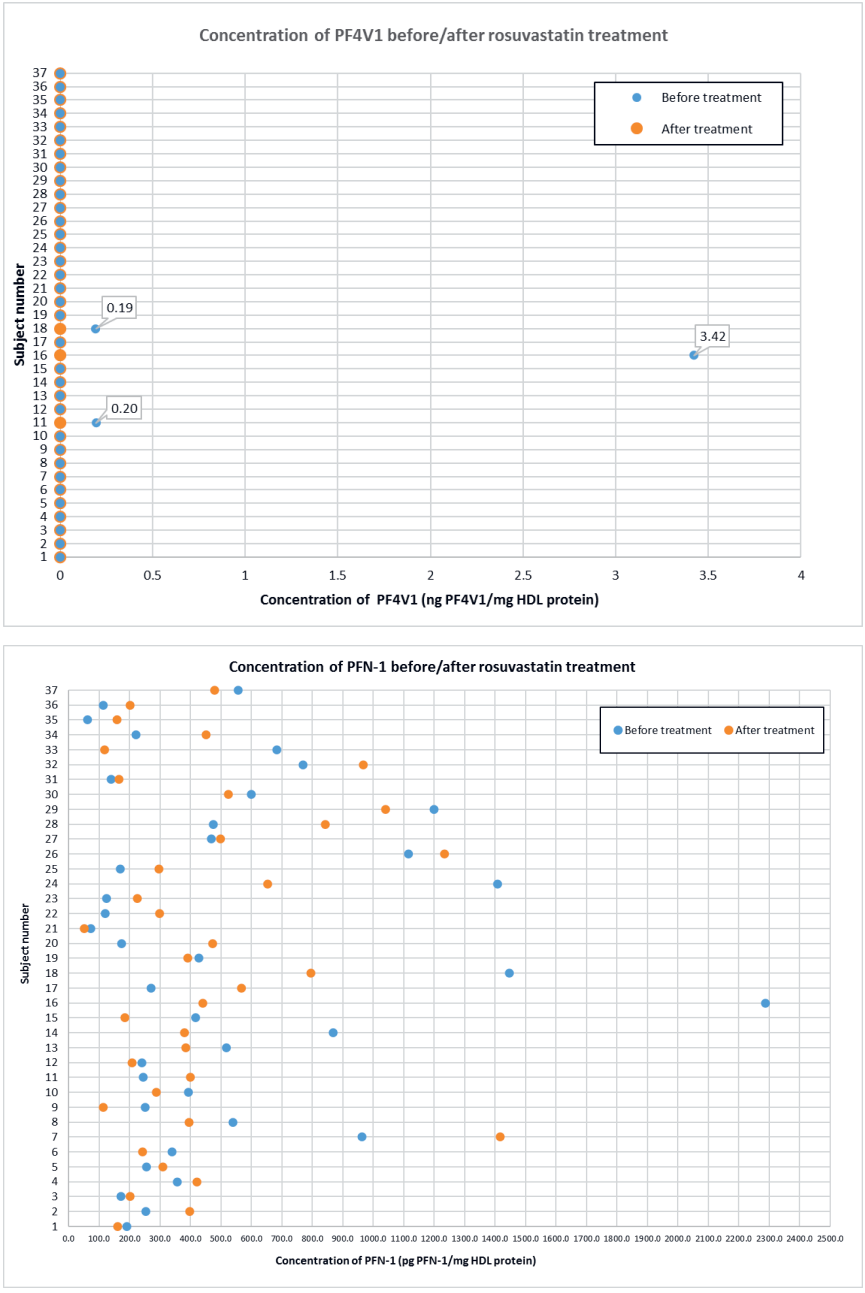

Fig. 5. Concentration of the validated HDL proteins before/after treatment: a) platelet factor 4 variant concentration before/after rosuvastatin treatment; b) Profilin-1 concentration before/after rosuvastatin treatment.

the obtained results in two, almost identical groups in size, *i.e.*, responders (patients who showed a decrease in Profilin-1 after treatment) and non-responders (patients who showed an increase of Profilin-1 after treatment). In order to assess whether the response of Profilin-1 to rosuvastatin treatment is dependent on any of the monitored clinical and biochemical parameters in the subjects, given in Supplementary Table SI, numerous correlations, univariate and multivariate analyzes were performed.

Pre-treatment Profilin-1 levels showed statistically significant associations with hsCRP, IL-6, IL-4, IL-10, and Interferon-γ (IFN-γ) (Table II). All associations were with positive Beta coefficients, *i.e.*, higher inflammatory marker levels were associated with higher levels of Profilin-1 prior to rosuvastatin treatment. The statistically significant associations with Profilin-1 were further analyzed with a multivariate linear regression-backward analysis (mean square of the model 81717.380; sig 0.000). In the last step of the model hsCRP and IL-6 remained to be independently associated with the Profilin-1 pre-treatment levels, with a positive association sign (Beta =.436, p = 0.001 and Beta =.393, p = 0.001, respectively).

Post-treatment Profilin-1 levels showed a statistically significant association only with hsCRP (Table III). The association was with a positive Beta coefficient, *i.e.*, higher concentrations of Profilin-1 in response to rosuvastatin treatment were correlated with higher hsCRP post-treatment levels, meaning that those subjects who had a smaller change in hsCRP levels, as a response to rosuvastatin, had increased concentrations of Profilin-1 in response to the treatment.

Post-treatment Profilin-1 levels showed statistically significant associations with the pre-treatment hsCRP and MCP-1 levels (Table IV). Both associations were with positive

Table II. Univariate linear regression analysis of Profilin-1 concentrations with hsCRP, IL-6, IL-4, IL-10 and IFN-γ levels before rosuvastatin treatment

Model		Unstandardized coefficients		Standardized coefficients	*t*	Sig.	95.0% C.I. for B	
		B	S.E.	Beta			Lower limit	Upper limit
1	(Constant)	245.886	73.605		3.341	.002	96.459	395.313
	hsCRP	77.392	13.588	.694	5.696	.000	49.806	104.977
1	(Constant)	443.911	62.611		7.090	.000	316.805	571.017
	IL-6	10.755	2.203	.636	4.881	.000	6.282	15.228
1	(Constant)	32.371	232.649		.139	.890	-439.932)	504.674
	IL-4	240.395	110.791	.344	2.170	.037	15.477	465.312
1	(Constant)	335.589	81.465		4.119	.000	170.206	500.972
	IL-10	222.182	59.083	.536	3.761	.001	102.238	342.126
1	(Constant)	441.829	63.030		7.010	.000	313.872	569.787
	IFN-γ	51.892	10.759	.632	4.823	.000	30.050	73.735

S.E. – standard error; CI – confidence interval

Table III. Univariate linear regression analysis of Profilin-1 concentrations with hsCRP levels after rosuvastatin treatment

Model		Unstandardized coefficients		Standardized coefficients	*t*	Sig.	95.0 % C.I. for B	
		B	S.E.	Beta			Lower limit	Upper limit
1	(Constant)	273.429	72.511		3.771	.001	126.224	420.633
	hsCRP	80.360	26.366	.458	3.048	.004	26.834	133.886

S.E. – standard error; CI – confidence interval

Table IV. Univariate linear regression analysis of post-treatment Profilin-1 concentrations with pre-treatment hsCRP and MCP-1 levels

Model		Unstandardized coefficients		Standardized coefficients	*t*	Sig.	95.0 % C.I. for B	
		B	S.E.	Beta			Lower limit	Upper limit
1	(Constant)	317.963	75.895		4.190	.000	163.888	472.037
	MCP-1	1.298	.601	.343	2.158	**.038**	.077	2.519
1	(Constant)	342.483	62.527		5.477	.000	215.547	469.418
	hsCRP	29.120	11.543	.392	2.523	.016	5.686	52.553

S.E. – standard error; CI – confidence interval

Beta coefficients, *i.e.*, the levels of both inflammatory markers, before rosuvastatin treatment, showed a direct proportional dependence of the post-treatment concentrations of Profilin-1. The two statistically significant associations were further analyzed with a multivariate linear regression-backward analysis (mean square of the model 65963.456; sig 0.001). In the last step of the model, only hsCRP remained to be independently associated with the Profilin-1 post-treatment levels, with a positive association sign (Beta =.391, $p = 0.007$).

From the multivariate regression, it can be concluded that the level of hsCRP, before rosuvastatin treatment, statistically significantly predicts the concentration of Profilin-1 after treatment ($F(3.33) = 7.172$, $p = 0.001$, $R^2 = 0.395$), ($p = 0.007$). Higher pre-treatment hsCRP levels are associated with higher post-treatment Profilin-1 concentrations.

In addition, if we look at the results of the association analysis of Profilin-1 concentrations before and after rosuvastatin treatment, the level of hsCRP constantly appears as a statistically significant predictor. Hence, it can be postulated that the concentration of Profilin-1 before and after treatment, *i.e.*, the response given by the concentration change (responders/non-responders) largely depends on the basal inflammatory phenotype of the subject (in our study expressed by the basal level of hsCRP), as well as the final inflammatory phenotype of the subject (expressed by the post-treatment level of hsCRP).

Limitations of the study

The small subject number might be a reason for possible omittance of statistically significant associations, that perhaps would appear with a larger cohort.

CONCLUSIONS

In summary, we evaluated the HDL proteome in a group of dyslipidemic subjects at low-to-moderate cardiovascular risk, without an established CVD, and tested whether rosuvastatin treatment alters the HDL proteome, thus possibly affecting its functionality. The comparative proteomic analysis identified 69 proteins, among which 10 new proteins were not previously known to be associated with HDL. A network analysis clustered the identified HDL proteins in four major functional groups, *i.e*., proteins involved in lipid transport and metabolism, proteins involved in platelet activation, coagulation, and hemostasis, proteins involved in the immune response, and proteins involved in the inflammatory and acute phase response. Rosuvastatin treatment led to decreased expressions of PF4V1 and PFN1. Although PF4V1 did not show differential abundance before and after treatment in the validation cohort using ELISA, the confirmed concentration reduction in 3 of the 37 tested samples is a promising direction for future studies investigating larger cohorts. The ELISA validation of PFN1 showed a segregation of the subjects, in terms of decreased/increased PFN1 levels after rosuvastatin, which was shown to be mostly dependent on the inflammatory milieu of the individual. Both findings present novel insights into the HDL proteome and the statins pleiotropism and open the door for future research.

Supplementary materials (Table SI and Table SII) are available upon request.

Acknowledgments. – The authors would like to thank the study participants for their contribution to the research endeavors.

Conflict of interest. – The authors declare that the research was conducted in the absence of any commercial or financial relationships that could be construed as a potential conflict of interest.

Funding. – This research did not receive any specific grant from funding agencies in the public, commercial, or not-for-profit sectors.

Authors contributions. – Conceptualization, project administration, supervision, quality check, A.V., A.D. and K.M.; data curation, A.V., M.V. and K.D.; formal analysis, A.V., K.D. and M.V.; investigation, software, and writing – original draft preparation, A.V., K.D., K.M. and M.V.; methodology, K.D.; resources, A.V., M.V. and K.M.; writing – review and editing, A.V., K.D., M.V., K.M. and A.D. All authors have read and agreed to the published version of the manuscript.

REFERENCES

1. F. L. J. Visseren, F. Mach, Y. M. Smulders, D. Carballo, K. C. Koskinas, M. Bäck, A. Benetos, A. Biffi, M. .J. Boavida, D. Capodanno, B. Cosyns, C. Crawford, C. H. Davos, I. Desormais, E. Di Angelantonio, O. Franco, S. Halvorsen, R. F. Hobbs, M. Hollander, E. Jankowska, M. Michal, S. Sacco, N. Sattar, L. Tokgozoglu, S. Tonstad, K. P Tsioufis, I. van Dis, I. van Gelder, C. Wanner and B. Williams, ESC Scientific Document Group. 2021 ESC Guidelines on cardiovascular disease prevention in clinical practice: Developed by the Task Force for cardiovascular disease prevention in clinical practice with representatives of the European Society of Cardiology and 12 medical soci-

eties with the special contribution of the European Association of Preventive Cardiology (EAPC), *Eur. Heart J.* **42**(34) (2021) 3227–3337; https://doi.org/10.1093/eurheartj/ehab484

2. F. Mach, C. Baigent, A. L. Catapano, K. C. Koskinas, M. Casula, L. Badimon, M. J. Chapman, G. G. De Backer, V. Delgado, I. M. Graham, A. Halliday, U. Landmesser, G. Riccardi, D. J. Richter, M. S. Sabatine, M. Taskinen, L. Tokgozoglu and O. Wiklund, ESC Scientific Document Group. 2019 ESC/EAS Guidelines for the management of dyslipidaemias: lipid modification to reduce cardiovascular risk: The Task Force for the management of dyslipidaemias of the European Society of Cardiology (ESC) and European Atherosclerosis Society (EAS), *European Heart Journal* **41**(1) (2020) 111–188; https://doi.org/10.1093/eurheartj/ehz455
3. A. J. Kattoor, N. V. K. Pothineni, D. Palagiri and J. Mehta, Oxidative stress in atherosclerosis, *Curr. Atheroscler. Rep.* **19** (2017) Article ID 42; https://doi.org/10.1007/s11883-017-0678-6
4. T. Senoner and W. Dichtl, Oxidative Stress in Cardiovascular Diseases: Still a Therapeutic Target?, *Nutrients* **11** (2019) Article ID 2090 (25 pages); https://doi.org/10.3390/nu11092090
5. J. Tuñón, M. Bäck, L. Badimón, M. Bochaton-Piallat, B. Cariou, M. J. Daemen, J. Egido, P. Evans, S. E. Francis, D. Ketelhuth, E. Lutgens, C. M. Matter, C. Monaco, S. Steffens, C. Weber and I. E. Hoefer, on behalf of the ESC Working Group on Atherosclerosis and Vascular Biology. Interplay between hypercholesterolaemia and inflammation in atherosclerosis: Translating experimental targets into clinical practice, *Eur. J. Prev. Cardiol.* **25**(9) (2018) 948–955; https://doi.org/10.1177/2047487318773384
6. K. B. Uribe, A. Benito-Vicente, C. Martin, F. Blanco-Vaca and N. Rotllan, (r)HDL in theranostics: how do we apply HDL's biology for precision medicine in atherosclerosis management? *Biomater. Sci.* **9** (2021) 3185–3208; https://doi.org/10.1039/D0BM01838D
7. C. B. Afonso and C. M. Spickett, Lipoproteins as targets and markers of lipoxidation, *Redox Biol.* **23** (2019) Article ID 101066 (16 pages); https://doi.org/10.1016/j.redox.2018.101066
8. S. Kajani, S. Curley and F. C. McGillicuddy, Unravelling HDL-looking beyond the cholesterol surface to the quality within, *Int. J. Mol. Sci.* **19**(7) (2018) Article ID 1971 (23 pages); https://doi.org/10.3390/ijms19071971
9. E. M. Stakhneva, E. V. Striukova and Y. I. Ragino, Proteomic studies of blood and vascular wall in atherosclerosis, *Int. J. Mol. Sci.* **22**(24) (2021) Article ID 13267 (17 pages); https://doi.org/10.3390/ijms222413267
10. J. C. Torres-Romero, J. C. Lara-Riegos, E. Parra, V. Sánchez, V. E. Arana-Argáez, S. Uc-Colli, M. Peña-Rico, M. A. Ramírez-Camacho, M. Regalado and M. E. Alvarez-Sánchez, *Lipoproteomics: Methodologies and Analysis of Lipoprotein-Associated Proteins along with the Drug Intervention*, in *Drug Design – Novel Advances in the Omics Field and Applications (Ed. A. A. Parikesit)*, IntechOpen, Jakarta 2020.
11. J. T. Wilkins and H. S. Seckler, HDL modification: recent developments and their relevance to atherosclerotic cardiovascular disease, *Curr. Opin. Lipidol.* **30**(1) (2019) 24–29; https://doi.org/10.1097/MOL.0000000000000571
12. W. S. Davidson, A. S. Shah, H. Sexmith and S. M. Gordon, The HDL Proteome Watch: Compilation of studies leads to new insights on HDL function, *Biochim. Biophys. Acta Mol. Cell Biol. Lipids* **1867**(2) **(**2022) Article ID 159072; https://doi.org/10.1016/j.bbalip.2021.159072
13. R. J. Havel, H. A. Eder and J. Bragdon, The distribution and chemical composition of ultracentrifugally separated lipoproteins in human serum, *J. Clin. Invest.* **34**(9) (1955) 1345–1353; https://doi.org/10.1172/JCI103182
14. E. de Juan-Franco, A. Pérez, V. Ribas, J. Sánchez-Hernández, F. Blanco-Vaca, J. Ordóñez-Llanos and J. Sánchez-Quesada, Standardization of a method to evaluate the antioxidant capacity of high-density lipoproteins, *Int. J. Biomed. Sci.* **5**(4) (2009) 402–410.

15. Y. Q. Yu, M. Gilar, P. J. Lee, E. Bouvier and J. Gebler, Enzyme-friendly mass spectrometry-compatible surfactant for in-solution enzymatic digestion of proteins, *Anal. Chem*. **75**(21) (2003) 6023–6028; https://doi.org/10.1021/ac0346196
16. K. Davalieva, S. Kiprijanovska, A. Dimovski, G. Rosoklija and A. J. Dwork, Comparative evaluation of two methods for LC-MS/MS proteomic analysis of formalin fixed and paraffin embedded tissues, *J. Proteomics* **235** (2021) Article ID 104117; https://doi.org/10.1016/j.jprot.2021.104117
17. J. C. Silva, R. Denny, C. Dorschel, M. Gorenstein, I. Kass, G. Z Li, T. McKenna, M. J. Nold, K. Richardson and P. Young, Quantitative proteomic analysis by accurate mass retention time pairs, *Anal. Chem*. **77**(7) (2005) 2187–2200; https://doi.org/10.1021/ac048455k
18. U. Distler, J. Kuharev, P. Navarro and S. Tenzer, Label-free quantification in ion mobility-enhanced data-independent acquisition proteomics, *Nat. Protoc*. **11** (2016) 795–812; https://doi.org/10.1038/nprot.2016.042
19. G. E. Ronsein and T. Vaisar, Deepening our understanding of HDL proteome, *Expert Rev. Proteomics* **16** (2019) 749–760; https://doi.org/10.1080/14789450.2019.1650645
20. W. S. Davidson, A. S. Shah, H. Sexmith and S. M. Gordon, The HDL proteome watch: Compilation of studies leads to new insights on HDL function, *Biochim. Biophys. Acta Mol. Cell. Bio.l Lipids* **1867**(2) (2022) Article ID 159072; https://doi.org/10.1016/j.bbalip.2021.159072
21. A. S. Shah, L. Tan, J. Long and W. S. Davidson, Proteomic diversity of high density lipoproteins: our emerging understanding of its importance in lipid transport and beyond, *J. Lipid Res*. **54**(10) (2013) 2575–2585; https://doi.org/10.1194/jlr.R035725
22. S. M. Gordon and A. T. Remaley, High density lipoproteins are modulators of protease activity: implications in inflammation, complement activation, and atherothrombosis, *Atherosclerosis* **259** (2017) 104–113; https://doi.org/10.1016/j.atherosclerosis.2016.11.015
23. Y. Yu, Y. Cui, Y. Zhao, S. Liu, G. Song, P. Jiao, B. Li, T. Luo, S. Guo, X. Zhang, H. Wang, X. Jiang and S. Qin, The binding capability of plasma phospholipid transfer protein, but not HDL pool size, is critical to repress LPS induced inflammation, *Sci. Rep*. **6** (2016) Article ID 20845 (12 pages); https://doi.org/10.1038/srep20845
24. A. S. Greene and S. L. Hajduk, Trypanosome lytic Factor-1 initiates oxidation-stimulated osmotic lysis of trypanosoma brucei brucei, *J. Biol. Chem*. **291**(6) (2016) 3063–3075; https://doi.org/10.1074/jbc.M115.680371
25. X. Xu, Y. Wang, C. M. Spring, J. Jin, H. Yang, M. Neves, P. Chen, Y. Yang, R. C. Gallant, J. Song, P. Ke, D. Zhang, N. Carrim, S. Yu, G. Zhu, Y. She, P. Chonelly, M. L. Rand, K. Adeli, J. Freedman, P. Marchese, W. S. Davidson, S. Jackson, C. Zhu and Z. Ruggeri, Apolipoprotein A-IV binds alphaI-Ibbeta3 integrin and inhibits thrombosis, *Nat. Commun*. **9**(3) (2018) Article ID 3608 (18 pages); https://doi.org/10.1038/s41467-018-05806-0
26. E. Reis, D. Mastellos, G. Hajishengallis and J. Lambris, New insights into the immune functions of complement, *Nat. Rev. Immunol*. **19** (2019) 503–516; https://doi.org/10.1038/s41577-019-0168-x
27. D. Alkam, E. Feldman, A. Singh and M. Kiaei, Profilin1 biology and its mutation, actin(g) in disease, *Cell Mol. Life Sci.* **74** (2017) 967–981; https://doi.org/10.1007/s00018-016-2372-1
28. A. Allen, D. Gau, P. Roy, The role of profilin-1 in cardiovascular diseases, *J. Cell Sci.* **134**(9) (2021) Article ID jcs249060 (11 pages); https://doi.org/10.1242/jcs.249060
29. E. Caglayan, G. Romeo, K. Kappert, M. Odenthal, M. Südkamp, S. Body, S. Shernan, D. Hackbusch and S. Rosenkranz, Profilin-1 is expressed in human atherosclerotic plaques and induces atherogenic effects on vascular smooth muscle cells, *PLoS One* **5**(10) (2010) e13608 (9 pages); https://doi.org/10.1371/journal.pone.0013608
30. G. Romeo, M. Pae, D. Eberlé, J. Lee and S. Shoelson, Profilin-1 haploinsufficiency protects against obesity-associated glucose intolerance and preserves adipose tissue immune homeostasis, *Diabetes* **62**(11) (2013) 3718–3726; https://doi.org/10.2337/db13-0050

31. B. Kasper and F. Petersen, Molecular pathways of platelet factor 4/CXCL4 signaling, *Eur. J. Cell Biol*. **90**(6–7) (2011) 521–526; https://doi.org/10.1016/j.ejcb.2010.12.002
32. L. Lasagni, R. Grepin, B. Mazzinghi, E. Lazzeri, C. Meini, F. Frosali, E. Ronconi, N. Alain-Courtois, L. Ballerini, G. Netti, F. Maggi, F. Annunziato, M. Serio, S. Romagnani, A. Bikfalvi and P. Romagnani, PF-4/CXCL4 and CXCL4L1 exhibit distinct subcellular localization and a differentially regulated mechanism of secretion, *Blood* **109**(10) (2007) 4127–4134; https://doi.org/10.1182/blood-2006-10-052035
33. J. Vandercappellen, J. Van Damme and S. Struyf, The role of the CXC chemokines platelet factor-4 (CXCL4/PF-4) and its variant (CXCL4L1/PF-4var) in inflammation, angiogenesis and cancer, *Cytokine Growth Factor Rev*. **22**(1) (2011) 1–18; https://doi.org/10.1016/j.cytogfr.2010.10.011
34. M. Gouwy, P. Ruytinx, E. Radice, F. Claudi, K. Van Raemdonck and S. Struyf, CXCL4 and CXCL4L1 Differentially Affect Monocyte Survival and Dendritic Cell Differentiation and Phagocytosis, *PLoS One* **11**(11) (2016) e0166006 (24 pages); https://doi.org/10.1371/journal.pone.0166006
35. K. Bledzka, S. Smyth and E. Plow, Integrin αIIbβ3: from discovery to efficacious therapeutic target, *Circ. Res*. **112**(8) (2013) 1189–1200; https://doi.org/10.1161/CIRCRESAHA.112.300570
36. E. Dupree, M. Jayathirtha, H. Yorkey, M. Mihasan, B. Petre and C. Darie, A critical review of bottom-up proteomics: The good, the bad, and the future of this field, *Proteomes* **8**(3) (2020) Article ID 14; https://doi.org/10.3390/proteomes8030014